Article

Cell Metabolism

Adiponectin Enhances Cold-Induced Browning of Subcutaneous Adipose Tissue via Promoting M2 Macrophage Proliferation

Graphical Abstract

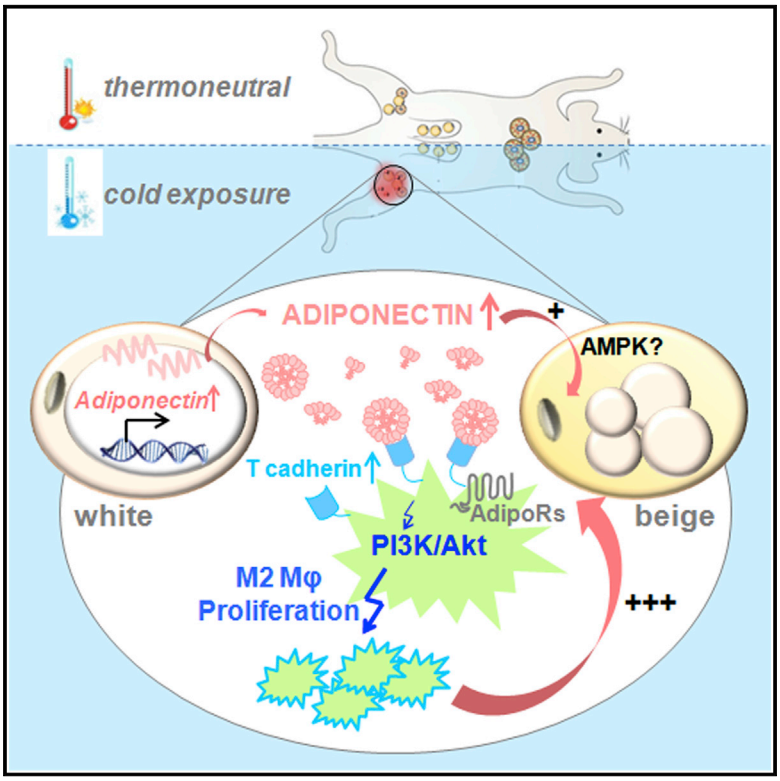

Authors

Xiaoyan Hui, Ping Gu, Jialiang Zhang, ..., Yu Wang, Karen S.L. Lam, Aimin Xu

Correspondence

amxu@hku.hk

In Brief

Adiponectin protects against a cluster of obesity-related metabolic complications through multiple mechanisms. This study shows that chronic cold exposure induces adiponectin accumulation in subcutaneous fat, which is indispensable for subcutaneous adipose browning via promoting M2 macrophage proliferation. These findings suggest a key role of adiponectin in mediating crosstalk between innate immunity and adaptive thermogenesis.

Highlights

- Cold exposure selectively induces adiponectin accumulation in subcutaneous WAT
- Adiponectin KO mice are resistant to subcutaneous adipose browning during cold adaptation
- Cold-induced M2 macrophage proliferation requires adiponectin in subcutaneous WAT
- T-cadherin serves as an anchor for tethering of adiponectin to M2 macrophages

Hui et al., 2015, Cell Metabolism *22*, 279–290
August 4, 2015
http://dx.doi.org/10.1016/j.cmet.2015.06.004

CellPress

Cell Metabolism
Article

Adiponectin Enhances Cold-Induced Browning of Subcutaneous Adipose Tissue via Promoting M2 Macrophage Proliferation

Xiaoyan Hui,[1,2,6] Ping Gu,[1,2,3,6] Jialiang Zhang,[1,2] Tao Nie,[4] Yong Pan,[1,2] Donghai Wu,[4] Tianshi Feng,[1,2] Cheng Zhong,[1,2] Yu Wang,[1,2,5] Karen S.L. Lam,[1,2] and Aimin Xu[1,2,5,*]
[1]State Key Laboratory of Pharmaceutical Biotechnology, The University of Hong Kong, Hong Kong 999077, China
[2]Department of Medicine, The University of Hong Kong, Hong Kong 999077, China
[3]Department of Endocrinology, Jinling Hospital/Nanjing General Hospital of Nanjing Military Command, Nanjing University School of Medicine, Nanjing 210093, China
[4]The Key Laboratory of Regenerative Biology, Guangzhou Institute of Biomedicine and Health, Chinese Academy of Sciences, Guangzhou 510530, China
[5]Department of Pharmacy and Pharmacology, The University of Hong Kong, Hong Kong 999077, China
[6]Co-first author
*Correspondence: amxu@hku.hk
http://dx.doi.org/10.1016/j.cmet.2015.06.004

SUMMARY

Adiponectin is an abundant adipokine with pleiotropic protective effects against a cluster of obesity-related cardiometabolic disorders. However, its role in adaptive thermogenesis has scarcely been explored. Here we showed that chronic cold exposure led to a markedly elevated production of adiponectin in adipocytes of subcutaneous white adipose tissue (scWAT), which in turn bound to M2 macrophages in the stromal vascular fraction. Chronic cold exposure-induced accumulation of M2 macrophages, activation of beige cells, and thermogenic program were markedly impaired in scWAT of adiponectin knockout (ADN KO) mice, whereas these impairments were reversed by replenishment with adiponectin. Mechanistically, adiponectin was recruited to the cell surface of M2 macrophages via its binding partner T-cadherin and promoted the cell proliferation by activation of Akt, consequently leading to beige cell activation. These findings uncover adiponectin as a key efferent signal for cold-induced adaptive thermogenesis by mediating the crosstalk between adipocytes and M2 macrophages in scWAT.

INTRODUCTION

The global surge in obesity prevalence, which results from a chronic imbalance between energy intake and energy expenditure, is posing serious health consequences, including type 2 diabetes, cardiovascular diseases, and many types of cancers. Several current anti-obesity drugs aiming to reduce food intake are found to be associated with severe psychiatric or cardiovascular side effects (Dietrich and Horvath, 2012). Therefore, alternative therapeutic strategies, such as by enhancing energy expenditure, are urgently needed to combat the obesity epidemic.

In contrast to white adipose tissue (WAT) that stores excess energy, brown adipose tissue (BAT) dissipates energy in the form of heat by uncoupling mitochondrial respiratory chain and ATP synthesis (Nedergaard et al., 2001). Besides classical brown adipocytes, which are mainly located in the interscapular fat depot, recent studies have identified a subset of cells within WAT that can be converted into brown-like adipocytes, called "beige" or "brite" (brown-in-white) adipocytes (Wu et al., 2012). In response to specific stimuli (such as cold exposure or β3 adrenergic receptor agonists), these otherwise quiescent beige cells undergo a "browning process" and adopt brown-like features, including multilocular lipid droplets and high UCP1 expression. Accumulating evidence from both animal and human studies suggests a therapeutic potential of beige cells in counteracting obesity and its related hepatic insulin resistance and chronic inflammation (Cohen et al., 2014; Cypess et al., 2009).

Although beige cells are morphologically and functionally similar to classical brown adipocytes, they are developmentally of different origins and are activated by overlapping, but distinct, mechanisms (Rosen and Spiegelman, 2014). The classical brown adipocytes share a common ancestor with myocytes that express *Myf5* and *Pax7* (Seale et al., 2008), whereas beige cells originate from a *Pax7*$^{-}$*Myf5*$^{-}$ lineage (Wu et al., 2012). Several secretory factors, such as prostaglandin, irisin, FGF21, and meteorin-like protein (Metrnl), are exclusive activators of beige cells but have no obvious effect on classical BAT (Rosen and Spiegelman, 2014). While norepinephrine from its sympathetic nerve terminals is the principal stimulator of cold-induced adaptive thermogenesis in classical BAT (Cannon and Nedergaard, 2004), the anti-inflammatory M2 macrophages serve as the important source of catecholamine for activation of beige cells within subcutaneous WAT (scWAT), which is less innervated but highly prone to browning in response to cold exposure (Qiu et al., 2014). Upon cold challenge or exercise, elevated Metrnl promotes the production of eosinophile-derived Th2 cytokines (IL-4 and IL-13), which in turn increases M2

macrophages, consequently leading to browning of scWAT (Rao et al., 2014). However, there are obvious differences in different WAT depots and species with respect to beige cell activity. The physiological relevance and the underlying mechanisms whereby the innate immune system participates in activation of beige cells and adaptive thermogenesis of WAT still remain obscure.

Adiponectin, one of the most abundant adipokines secreted from adipocytes, possesses pleiotropic salutary effects against a cluster of obesity-related disorders, including insulin resistance, fatty liver, cardiovascular diseases, depression, and cancers (Kadowaki et al., 2006). Adiponectin exerts its multiple actions via its seven-transmembrane receptors, adipoR1 and adipoR2 (Yamauchi et al., 2003). T-cadherin, a plasma membrane-anchored glycoprotein, has also been implicated in tethering the high molecular weight (HMW) form of adiponectin at the cell surface and transducing adiponectin actions in several tissues (Denzel et al., 2010; Hug et al., 2004; Parker-Duffen et al., 2013). Besides its endocrine actions in heart and skeletal muscle, adipose tissue is also a target of adiponectin, where it increases insulin sensitivity and counteracts obesity-induced macrophage infiltration and inflammation (Kim et al., 2007). Notably, adiponectin promotes the polarization of macrophages toward the anti-inflammatory M2 phenotype in WAT (Mandal et al., 2011). However, whether the effects of adiponectin in macrophage polarization are functionally relevant to beige cell activation in WAT has not been explored. Unlike most of the adipokines, adiponectin is contradictorily downregulated in the context of obesity in both rodents and humans (Arita et al., 1999), although the cause-effect relationship between hypoadiponectinemia and obesity remain elusive.

In this current study, we explored the potential role of adiponectin in adaptive thermogenesis. We found that cold exposure induced a selective and drastic elevation in *Adiponectin* mRNA expression (>300-fold) as well as adiponectin protein in mouse scWAT, but not in classical interscapular BAT and epididymal WAT (eWAT). Importantly, adiponectin knockout (ADN KO) mice displayed blunted activation of beige cells within scWAT in response to chronic cold exposure, whereas the thermogenic activity in BAT was unaffected. Therefore, we further investigated the mechanisms whereby adiponectin mediates cold-induced browning of scWAT via regulation of M2 macrophages.

RESULTS

Chronic Cold Exposure Selectively Induced Accumulation of Adiponectin in Subcutaneous WAT

In order to explore the potential roles of adiponectin in cold-induced thermogenesis, we housed C57BL/6J male mice at 6°C for various time periods, and circulating levels of adiponectin and its expression in different adipose depots were examined. Consistent with a previous report (Dong et al., 2013), there was a modest decline in serum level of adiponectin compared to those housed at the thermal neutral condition (30°C) (Figure S1A). However, quantitative real-time PCR analysis showed that *Adiponectin* mRNA was elevated in scWAT as early as 6 hr after cold exposure, and the induction was more drastic (>300-fold) after prolonged cold acclimation, including 6 days and 1 month (Figure 1A), and this change was accompanied by an obvious increase in adiponectin protein in subcutaneous WAT (scWAT) (Figures 1B and 1C). Notably, in contrast to the changes in scWAT, the expression of adiponectin was not obviously altered by cold temperature in either epididymal WAT (eWAT) or interscapular BAT (Figures S1B and S1C).

To further verify the above findings, adiponectin knockout (ADN KO) mice were housed at 30°C or 6°C for 2 days, followed by administration of fluorescently labeled adiponectin by intravenous tail vein injection. The distribution of exogenous adiponectin was monitored by fluorescence imaging. Both in vivo imaging (Figures 1D and 1E) and fluorescence analysis in various organs (Figures 1F and 1G) demonstrated that cold exposure led to a selective enrichment of adiponectin in scWAT, but not in other tissues, including BAT, eWAT, liver, and kidney. The sequestration of intravenously injected adiponectin into scWAT under the cold condition was also confirmed by immunohistochemical staining of adiponectin (Figure 1H).

Adiponectin Knockout Mice were Resistant to Cold-Induced Browning in scWAT

We next examined the impact of adiponectin deficiency on cold-induced thermogenesis in both scWAT and interscapular BAT. Real-time PCR analysis revealed that prolonged cold exposure led to a marked induction of *Ucp1* and other key thermogenic genes in scWAT of wild-type (WT) mice (Figure 2A). Interestingly, these changes were markedly mitigated in ADN KO mice (Figure 2A). Immunohistochemical analysis showed that cold exposure induced the formation of multilocular, brown-like adipocytes in scWAT of both the inguinal and back depots in WT mice, but such a browning effect of cold exposure was dramatically impaired in ADN KO mice (Figures 2B and S2A). Likewise, a marked impairment in cold-induced expression of UCP1 protein in scWAT of ADN KO mice was also detected by western blot analysis (Figure 2C). Intriguingly, the interscapular BAT of ADN KO and WT mice exhibited a similar level of UCP1 expression after chronic cold challenge (Figure S2B), suggesting that the effect of adiponectin on adaptive thermogenesis was specific to scWAT.

By using the Seahorse XFe24 analyzer, the total and UCP1-dependent oxygen consumption rate (OCR) was quantified in various adipose depots from WT and ADN KO mice after 6 days of cold challenge. The OCR rate in scWAT was comparable between ADN KO mice and WT littermates when being housed at the thermoneutral condition (Figure 2D). As expected, chronic cold exposure significantly increased both basal and NE-stimulated OCRs in scWAT, whereas such an effect was largely abrogated in ADN KO mice (Figure 2D). Furthermore, cold-induced UCP1-dependent OCR, as calculated by the difference between NE and GDP-treated OCR, was remarkably suppressed in ADN KO mice compared to WT littermates (Figure 2E). In contrast, BAT of WT and ADN KO mice displayed comparable levels of OCR under both thermoneutral and cold conditions (Figures S2C and S2D). The whole-body oxygen consumption (VO_2), as determined by comprehensive laboratory animal monitoring system (CLAMS) analysis, was comparable between ADN KO and WT mice housed at the ambient temperature, whereas ADN KO mice displayed a modest, but significant, reduction in cold-induced elevation of oxygen consumption after 6 days of acclimation to 6°C (Figures 2F and 2G).

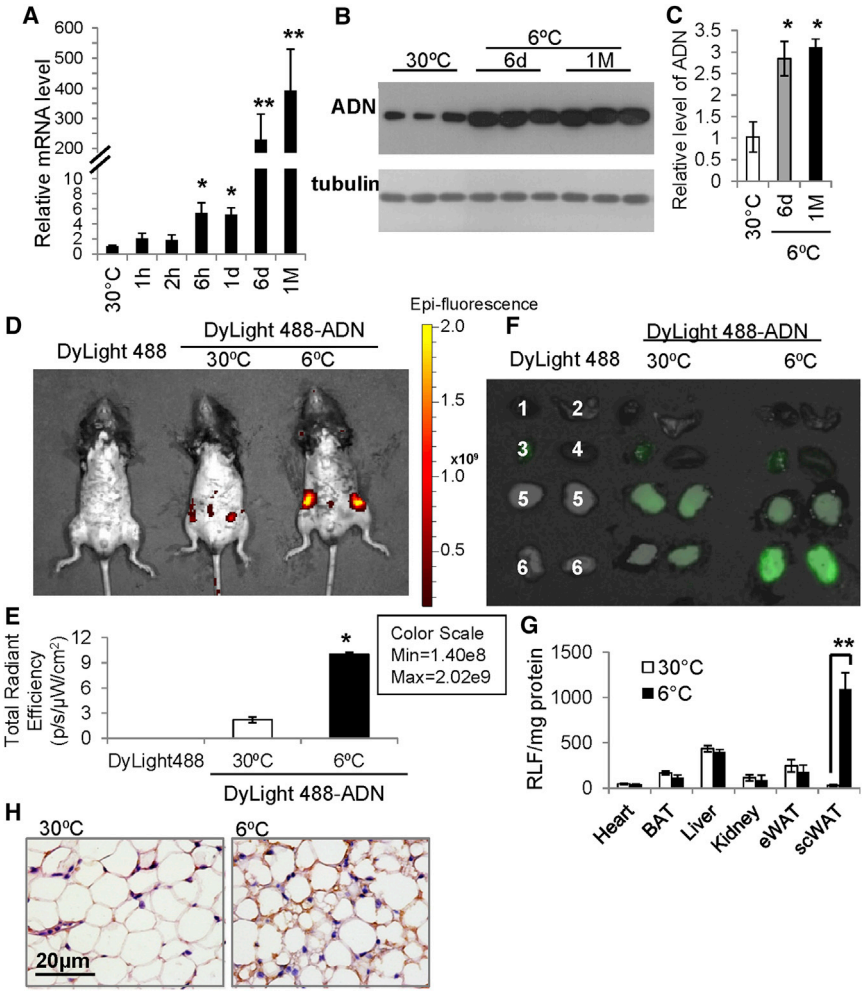

Figure 1. Chronic Cold Exposure Markedly Induced Accumulation of Adiponectin in scWAT

(A–H) 10-week-old C57BL/6J mice were housed at 6°C for various time periods or at thermoneutral condition (30°C) as control. (A) Real-time PCR and (B) western blot analysis for adiponectin (ADN) mRNA and protein levels in scWAT, respectively. (C) Densitometry quantification of western blot results of ADN relative to tubulin. (D–G) Adiponectin knockout (ADN KO) mice were housed at 30°C or 6°C for 2 days, followed by intravenous injection of 50 μg of fluorescently labeled adiponectin or Dylight488 only (with equal fluorescence intensity) as control. (D) The mice and (F) their various tissues were subjected to in vivo fluorescence imaging analysis 1 hr post-injection. 1, heart; 2, BAT; 3, liver; 4, kidney; 5, eWAT; 6, scWAT. (E) Quantification of fluorescence intensity in inguinal region of the mice and (G) various tissues. (H) Inguinal scWAT was collected 1 hr after ADN KO mice housed in either 30°C or 6°C were injected with 50 μg of unlabeled recombinant adiponectin. Immunochemical staining of adiponectin in scWAT of ADN KO mice (scale bar, 20 μm). Data represent mean ± SEM; n = 3 independent experiments; 6–8 mice for each experiment; *p < 0.05, **p < 0.01 versus 30°C. See also Figure S1.

Cold-Induced Enrichment of Anti-inflammatory M2 Macrophages in scWAT Was Dependent on Adiponectin

To further address how adiponectin contributes to cold-evoked browning in scWAT, we first investigated whether adiponectin possesses a direct browning capacity, similar to FGF21 and irisin. To this end, stromal vascular fraction (SVF) of scWAT was isolated and differentiated to mature adipocytes, followed by incubation with recombinant adiponectin for 24 hr. This analysis showed that adiponectin induced *Ucp1* gene expression in a concentration-dependent manner (Figure S3A). The in vitro effects of adiponectin on induction of UCP1 were abrogated by the AMP-activated protein kinase (AMPK) inhibitor compound c, but not by the p38 MAPK inhibitor SB203580 (Figure S3B), suggesting that adiponectin-mediated activation of AMPK may contribute to its induction of *Ucp1* expression. However, no significant elevation of UCP1 protein was observed in adiponectin-treated adipocytes (Figure S3C). Therefore the modest direct effect of adiponectin on browning of white adipocytes seems unable to fully explain the marked differences in cold-evoked beige cell activation between WT and ADN KO mice. We thus explored whether there exist additional mechanism(s) accounting for adiponectin-induced adipose tissue browning.

It was recently reported that M2 macrophages enhance thermogenic remodeling in scWAT by producing catecholamine (Qiu et al., 2014). Indeed, quantitative real-time PCR analysis demonstrated that *F4/80* and markers of M2 macrophages were steadily elevated upon chronic cold exposure (Figures S4A and S4B). Although *iNOS*, a marker of M1 macrophage, was also induced, the induction fold was much less than those of M2 markers after 6 days of cold challenge and decreased afterward (Figure S4B). In contrast to the dramatic increase of M2 macrophages in scWAT, such changes were not observed in BAT and eWAT (data not shown). Consistently, flow cytometry analysis of the SVF from scWAT demonstrated a significantly elevated accumulation of F4/80^{+} cells from mice housed for 6 days at 6°C (Figure S4C). This cold-induced change was accompanied by increased composition of M2 macrophages (cd11c^{low}cd206^{high}), while the composition of M1 macrophages (cd11c^{high}cd206^{low}) remained constant (Figure S4C), confirming that cold challenge caused a strong and specific enrichment of M2 macrophages within scWAT.

In order to evaluate the roles of M2 macrophage in scWAT browning, we depleted macrophages in scWAT by injecting the clodronate-conjugated liposome (CLOD) into C57BL/6J mice, followed by exposure at 6°C for 48 hr. The successful depletion of macrophages was verified by flow cytometry analysis (Figure S4D) and real-time PCR (Figure S4E). Notably, cold-induced expression of thermogenic genes was abrogated in scWAT of macrophage-depleted mice (Figures S4F–S4H), whereas the thermogenic genes in BAT remained unaffected

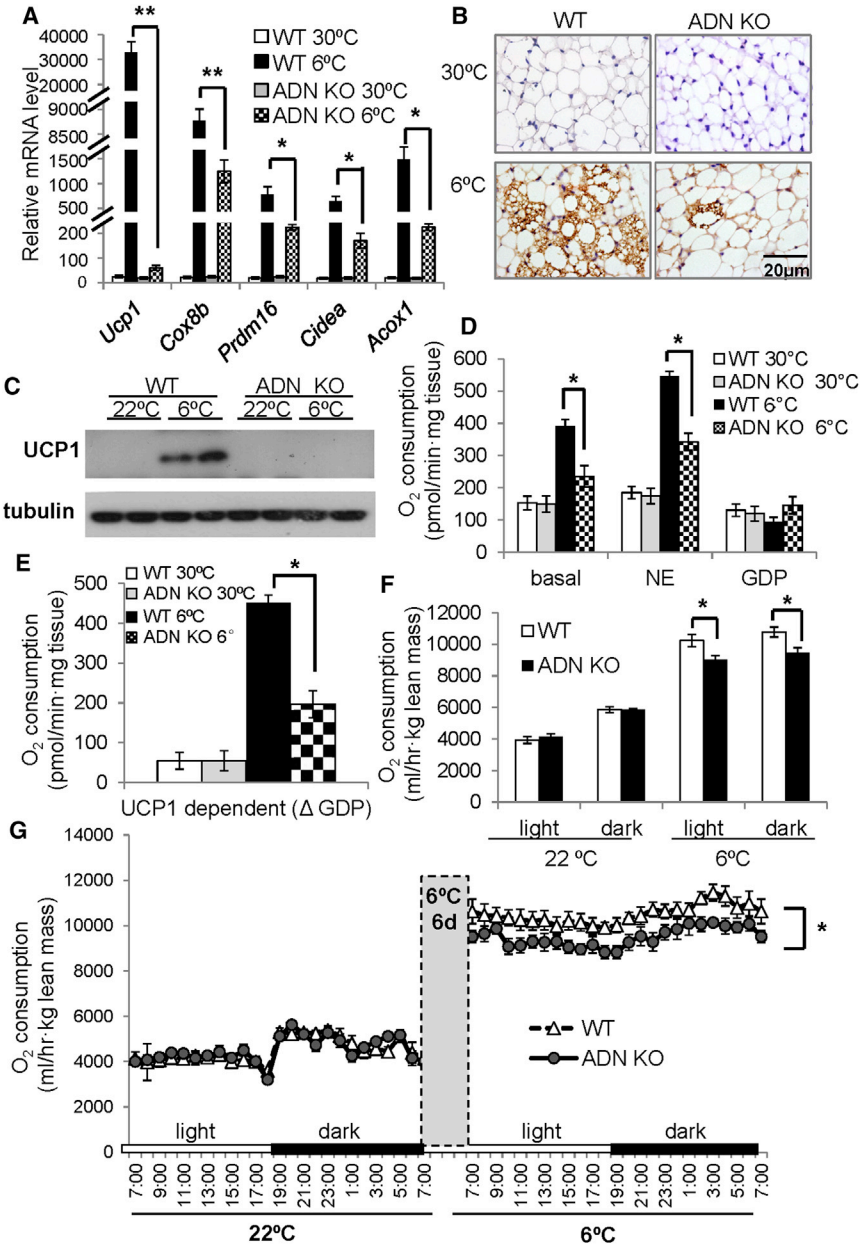

Figure 2. ADN KO Mice Were Refractory to Cold-Induced Browning in scWAT

(A–G) ADN KO and wild-type (WT) littermates with C57BL/6J background were housed at 6°C or 30°C (or 22°C) for 6 days. (A) Real-time PCR analysis for mRNA abundance of *Ucp1* and other markers for brown adipocytes, including *Cox8b*, *Prdm16*, *Cidea*, and *Acox1*. (B) Immunohistochemistry (scale bar, 20 μm) and (C) western blot analysis of UCP1 protein expression in scWAT. (D) Basal, NE, and GDP-stimulated oxygen consumption rate (OCR) and (E) UCP1-dependent OCR in scWAT as calculated by the difference between NE and GDP-treated OCR. (F and G) Whole-body oxygen consumption in WT and ADN KO mice (F) during a day/light cycle and (G) in a 24 hr period. Data are mean ± SEM; n = 4 independent experiments; 8 mice for each experiment; *p < 0.05, **p < 0.01. See also Figure S2.

(Figure S4I). Macrophage depletion did not affect cold-induced elevation of adiponectin expression in scWAT (Figure S4J), suggesting that adiponectin acts at the upstream of macrophage accumulation during cold-induced scWAT remodeling.

We next examined the roles of adiponectin in cold-induced M2 macrophage accumulation in scWAT. To this end, mature adipocytes and SVF were isolated from scWAT, and adiponectin in each fraction was examined by western blotting. At the thermoneutral condition, adiponectin protein was predominantly present in mature adipocytes and barely detectable in SVF (Figure 3A). On the other hand, prolonged cold exposure led to a greater than 3-fold elevation in adiponectin protein levels in SVF, whereas there was only a modest, but statistically insignificant, elevation of adiponectin in mature adipocyte fraction (Figures 3A and 3B). By contrast, cold-induced mRNA expression of the *Adiponectin* gene was detected predominantly in the mature adipocytes, whereas *Adiponectin* mRNA was virtually undetectable in the SVF under both warm and cold conditions (Figure 3C), indicating that the adiponectin protein detected in the SVF cells was produced and transported from the adipocytes.

We next investigated whether cold-induced accumulation of adiponectin in the SVF of scWAT plays a role in modulating sequestration of M2 macrophage in this compartment. Both real-time PCR analysis and flow cytometry showed that cold exposure-induced M2 macrophage accumulation in scWAT was largely abolished in ADN KO mice (Figures 3D and 3E). On the other hand, replenishment with recombinant adiponectin reversed the impairment in cold-induced accumulation of M2 macrophages and UCP1 expression in ADN KO mice but had little effect on UCP1 expression in interscapular BAT (Figure 4). Supplementation of the β3-adrenergic receptor agonist CL316,243 completely reversed the impairment in cold-induced browning in ADN KO mice (Figure 5), indicating that adiponectin deficiency does not affect the progenitor cells for browning in scWAT. Taken together, these findings suggest that adiponectin is obligatory for cold-induced enrichment of M2 macrophages, which in turn promotes browning of scWAT.

Adiponectin Deficiency Had No Obvious Effect on Expression of Type 2 Cytokines and Abundance of ILC2s in scWAT

Th2 cytokines are the important mediators of cold-induced beige cell formation by promoting polarization of macrophage to the M2 subtype (Qiu et al., 2014; Rao et al., 2014). We therefore

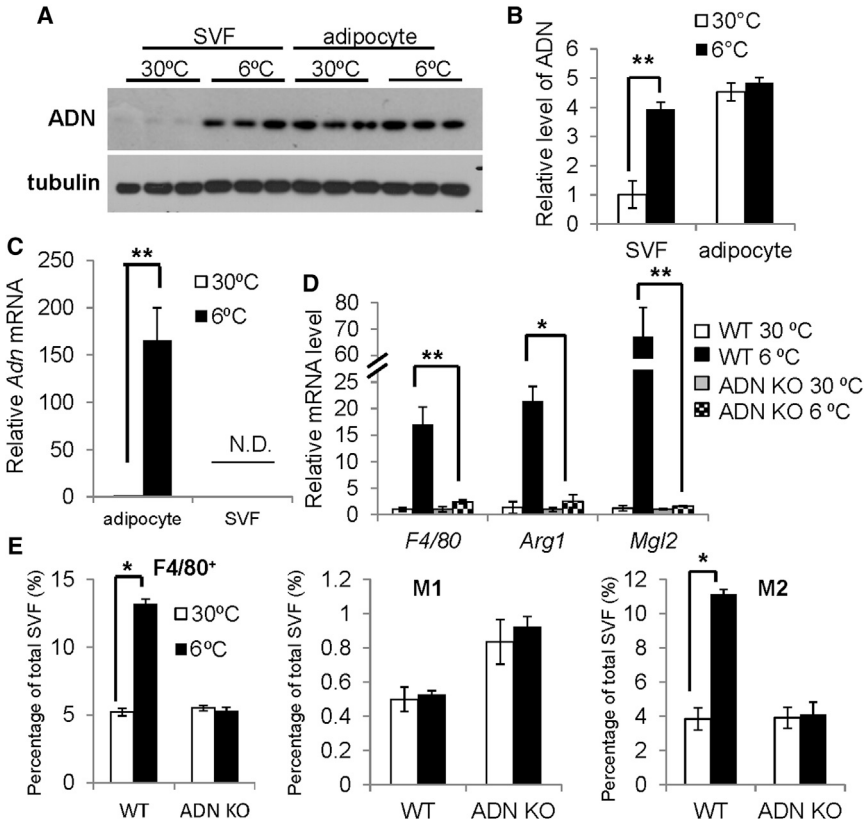

Figure 3. Cold-Induced Accumulation of Adiponectin Was Required for Enrichment of M2 Macrophages in scWAT

(A–C) 10-week-old C57BL/6J male mice were housed at 6°C or 30°C for 6 days, followed by fractionation of inguinal scWAT into mature adipocytes and stromal vascular fraction (SVF). (A) Representative image of western blot. (B) Densitometry analysis of results in (A). (C) Real-time PCR analysis for relative mRNA abundance, respectively. N.D., not detected.

(D and E) Inguinal scWAT of 10-week-old ADN KO mice and WT littermates housed at 6°C or 30°C for 6 days were subjected to real-time PCR analysis for (D) mRNA levels of *F4/80*, *Arg1*, and *Mgl2* and (E) flow cytometry analysis for total, M1, and M2 macrophages. Data represent mean ± SEM; n = 4 independent experiments; 6 mice for each experiment; *p < 0.05, **p < 0.01. See also Figure S3.

determined whether adiponectin modulates M2 macrophages through the Th2 cytokines. Real-time PCR analysis demonstrated that the expression of *IL-4* and *IL-13* was acutely induced in scWAT of both ADN KO and WT mice at 6 hr and 24 hr after cold challenge, but reduced significantly after prolonged cold exposure for 6 days (Figures S5A and S5B). The dynamic changes of *IL-4* and *IL-13* expression were comparable between ADN KO mice and WT littermates.

We next investigated the effect of adiponectin on group 2 innate lymphoid cells (ILC2s) and ILC2-derived cytokines, which have recently been reported to contribute to de novo expansion of beige fat under obese conditions (Brestoff et al., 2015). The expression levels of the *IL-33* and thymic stromal lymphopoietin (*TSLP*), both of which are ILC2 activators, were unaltered at day 1 after cold challenge (Figures S5C and S5D). *TSLP* expression was decreased significantly after 6 days of cold exposure. The expression of *IL-5* and Proenkephalin (*Penk*), which are the two ILC2-secreted factors involved in beige cell formation, was elevated at the first day after cold challenge but decreased after prolonged cold exposure (Figures S5E and S5F). Flow cytometry analysis showed that the changes in the number of ILC2s, which were defined as Lin^-, $CD45^+$, $CD25^+$, and $IL33R^+$, in the SVF of scWAT mirrored those of *TSLP* (Figures S5G and S5H). There was no difference in either expression levels of *IL-33*, *IL-5*, *TSLP*, and *Penk* or abundance of ILC2s between ADN KO mice and WT littermates under both warm and cold conditions. These data suggest that Th2 cytokines and ILC2s and its derived factors are not the direct downstream targets of adiponectin.

M2 Macrophages Underwent De Novo Proliferation in scWAT upon Cold Challenge in WT, but Not in ADN KO Mice

To investigate how adiponectin promotes cold-induced M2 macrophage accumulation in scWAT, we first examined whether cold challenge-induced accumulation of M2 macrophages were derived from circulating monocytes as in obese state (Oh et al., 2012). To this end, circulating monocytes were isolated from peripheral blood of the donor C57BL/6J mice, labeled with the fluorescent dye PKH26, and delivered to recipient mice via tail vein injection. The presence of these fluorescently labeled monocytes was monitored by flow cytometry (Figure S6A). By this in vivo macrophage/monocyte tracking method, we found that cold challenge did not alter the incorporation rate of the PKH26-positive monocytes in scWAT, eWAT, or spleen (Figure S6B) or the decline rate of the labeled monocytes in the circulation (Figure S6C), suggesting that cold-induced elevation of M2 macrophages in scWAT is not attributed by the infiltration of circulating monocytes.

Accumulating evidence suggests that tissue-resident macrophages are maintained by local self-renewal in a manner independent of circulating monocytes (Hashimoto et al., 2013; Robbins et al., 2013). We thus examined whether the cold-induced accumulation of M2 macrophages depends on local macrophage proliferation. To this end, C57BL/6J mice housed at either 30°C or 6°C were subcutaneously injected with the thymidine analog EdU to tag the dividing cells, followed by quantification of the proliferating cells labeled with EdU using flow cytometry. This analysis showed that only 1.9% ± 0.5% of M2 macrophages in SVF obtained from scWAT, identified as $F4/80^+cd206^{high}cd11c^{low}$, were stained positive for EdU when mice were being housed at the thermoneutral condition (Figures 6A and 6B). Notably, chronic cold exposure significantly elevated the percentage of EdU^+M2 macrophages (6.9% ± 0.6%) in scWAT, but not in eWAT (Figure 6A). However, cold-induced M2 macrophage proliferation in scWAT was abrogated in ADN KO mice (Figures 6A and 6B).

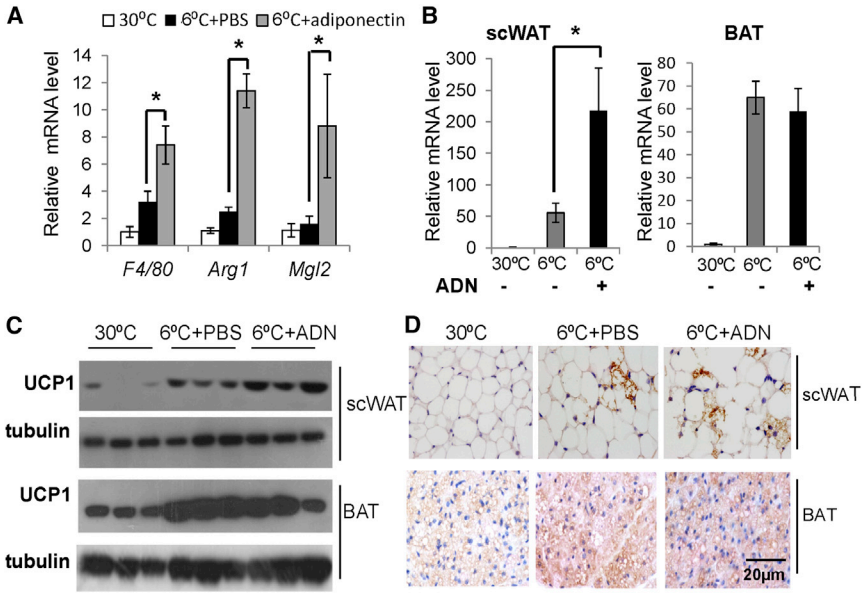

Figure 4. Supplementation of Adiponectin Reversed the Impairment in Cold-Induced M2 Macrophage Accumulation and Browning in scWAT of ADN KO Mice

(A–D) 10-week-old male ADN KO mice with C57BL/6J background housed at 6°C were treated with PBS or recombinant adiponectin by intravenous injection (2.5 mg/kg/day) for 6 days. (A and B) The mRNA levels of (A) *F4/80* and (B) M2 macrophage markers (*Arg1* and *Mgl2*) in scWAT as determined by real-time PCR. (B) Real-time PCR, (C) western blot, and (D) immunohistochemistry analysis for UCP1 mRNA and protein levels, respectively, in scWAT and BAT (scale bar, 20 μm). Data represent mean ± SEM; n = 3 independent experiments; 6 mice for each experiment; *p < 0.05.

Adiponectin Directly Promoted M2 Macrophage Proliferation In Vitro

To investigate the direct effect of adiponectin on macrophage proliferation, bone marrow-derived macrophages were first polarized to M1 or M2 subtypes, followed by treatment with recombinant adiponectin. Both real-time PCR and immunocytochemical analysis demonstrated that adiponectin caused a significant induction of Ki67 expression in M2 macrophages, but not in M1 macrophages (Figures 6C–6F). EdU incorporation assay also confirmed that the proliferation of M2 macrophages, but not M1 macrophages, was enhanced by addition of adiponectin (Figures 6G and 6H).

The phosphatidylinositide 3-kinase (PI3K)-Akt signaling pathway has been shown to mediate the effects of IL-4 on proliferation of tissue-resident M2 macrophages (Rückerl et al., 2012). Notably, adiponectin induced a significant elevation of Akt phosphorylation (S473) in M2 macrophages, but not in M1 macrophages (Figure 6I). Furthermore, pharmacological inhibition of PI3K with Ly29004 or Akt with MK-2206 largely blocked the effect of adiponectin on M2 macrophage proliferation (Figure 6J).

Adiponectin exerts its actions by binding to its two receptors AdipoR1 and AdipoR2 (Kadowaki et al., 2006). In addition, high molecular weight (HMW) and hexameric form of adiponectin binds to T-cadherin, a cell surface-anchored glycoprotein that in turn traps adiponectin within the tissues (Denzel et al., 2010; Hug et al., 2004). We next investigated the involvement of these adiponectin receptors in adiponectin-mediated M2 macrophage proliferation in scWAT in response to cold challenge. The dramatic elevation of adiponectin in scWAT upon cold challenge was accompanied by an obvious increase in expression of *T-cadherin*, whereas the expression of *adipoR1* and *adipoR2* remained unchanged (Figure 7A). Interestingly, the expression of *T-cadherin* in M2 macrophages was much higher than in M1 macrophages, while the expression of *adipoR1* and *adipoR2* were comparable between M1 and M2 macrophages (Figure 7B). Knockdown of T-cadherin by siRNA (Figure 7C) significantly reduced the binding of adiponectin to the surface of M2 macrophages, as determined by immunocytochemistry (Figure 7D). Moreover, adiponectin-induced proliferation of M2 macrophages, as evidenced by upregulation of *Ki67* and incorporation of EdU, was largely abrogated by knockdown of T-cadherin (Figures 7E–7G). Taken together, these findings suggest that elevated T-cadherin serves as an anchor to tether adiponectin in scWAT, which in turn promotes M2 macrophage proliferation in response to cold challenge.

DISCUSSION

Despite extensive research on adiponectin in the past decade, its role in adaptive thermogenesis has scarcely been explored. This study provides a series of evidence that adiponectin is an obligatory mediator of cold-induced browning of WAT. Chronic cold exposure leads to markedly elevated mRNA expression as well as increased accumulation of adiponectin protein in scWAT, which in turn activates the thermogenic program by its direct actions in adipocytes or/and promoting in situ proliferation of M2 macrophages. The selective accumulation of adiponectin in scWAT, but not eWAT, may explain in part why scWAT is more prone to browning compared with eWAT.

As one of the most abundant adipokines in the body, the pleiotropic role of adiponectin has been implicated in almost all the tissues and cell types throughout the body. Although predominantly expressed in mature adipocytes, the sequestration of circulating adiponectin into injured tissues (such as blood vessels, liver, and heart) has been observed in several pathological conditions (Denzel et al., 2010; Lin et al., 2014; Nakatsuji et al., 2014; Parker-Duffen et al., 2013). Under these circumstances, locally accumulated adiponectin serves as a defense mechanism to prevent its surrounding areas from further damage, such as atherosclerotic lesion, myocardial infarction, and liver necrosis. Additionally, bone marrow adipose tissue in mice on a restricted diet has been reported to be a major source of circulating adiponectin, which in turn facilitates adaption of skeletal muscle to calorie restriction (Cawthorn et al., 2014). In the current study, we observed a >300-fold increase in mRNA expression and approximately 3-fold elevation in protein abundance of

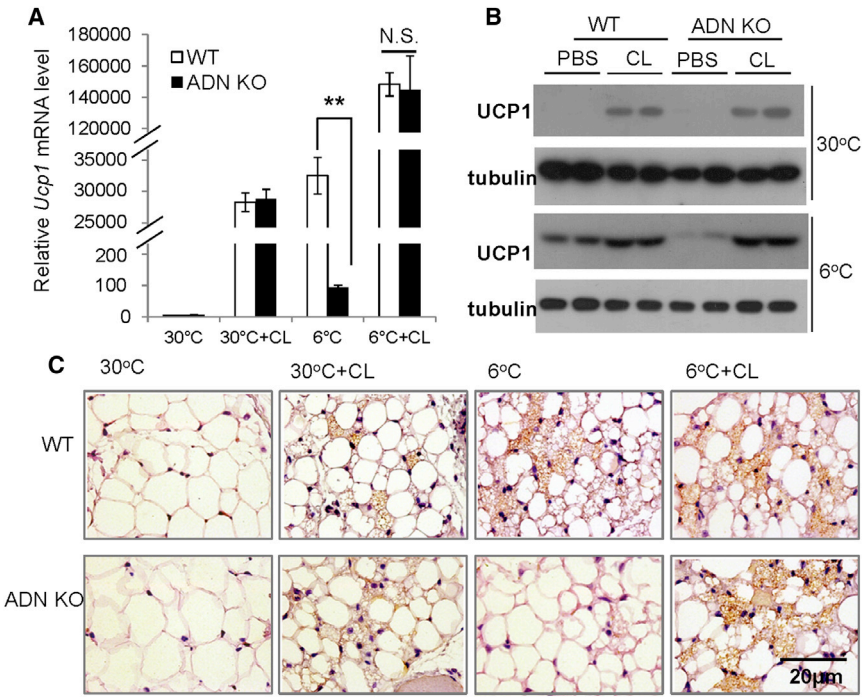

Figure 5. The Defect in Cold-Induced Browning of scWAT in ADN KO Mice Was Reversed by Replenishment of CL316,243

(A–C) 10-week-old male WT and ADN KO mice with C57BL/6J background housed at 30°C or 6°C were intraperitoneally administered with CL316,243 (0.5 mg/kg body weight/day) or PBS as vehicle for 6 days. The mRNA and protein abundance of UCP1 in scWAT was determined by (A) real-time PCR, (B) western blotting, and (C) immunohistochemical staining (scale bar, 20 μm). Data are mean ± SEM; n = 3 independent experiments; 6 mice for each experiment; **p < 0.01. See also Figure S4.

adiponectin in scWAT, but not in eWAT and BAT in response to chronic cold exposure. The discordant changes between mRNA and protein levels of adiponectin are possibly due to the low efficiency of protein biosynthesis in the cold temperature. Notably, cold-induced accumulation of adiponectin is located predominantly in the SVF, perhaps due to the upregulated expression of T-cadherin (a cell surface-anchored glycoprotein with adiponectin-binding properties) in adipose-resident macrophages. In support of this notion, our in vitro analysis demonstrated that knockdown of T-cadherin in cultured M2 macrophages significantly abolished the tethering of adiponectin to the cell surface, concomitant with a compromised effect of adiponectin on promoting macrophage proliferation. These findings are reminiscent of the aforementioned scenarios observed in injured tissues in that adiponectin was locally accumulated in stressed aorta, heart, kidney, and lung in a T-cadherin-dependent manner (Denzel et al., 2010; Nakatsuji et al., 2014; Parker-Duffen et al., 2013). Moreover, in obese adipose tissue, adiponectin is selectively elevated in SVF and surrounds macrophages, despite a decreased circulating adiponectin (Nakatsuji et al., 2014).

It is currently unclear why cold exposure leads to a selective upregulation of T-cadherin and elevation of adiponectin in scWAT, but not in eWAT and classical BAT. One possible explanation is the superficial location of scWAT, which allows it to directly serve as a thermal sensor and thus turns on the "cold-responsive" genes in a β-adrenergic receptor-independent manner (Ye et al., 2013). Notably, cold exposure has been shown to induce the production of reactive oxygen species (ROS) in cultured cells (Awad et al., 2013). ROS can directly induce the expression of T-cadherin (Joshi et al., 2005), possibly via a ROS-sensitive regulatory element with the promoter region.

Although our in vitro experiment showed a significant effect of adiponectin on induction of *Ucp1* gene in an AMPK-dependent manner in scWAT-derived adipocytes, there was no obvious elevation in UCP1 protein, indicating that the direct actions of adiponectin in adipocytes are unlikely to be the major contributor to adiponectin-induced browning of scWAT. Instead, our data suggest that the browning effects of adiponectin in scWAT are mainly attributed to its ability in mediating cold-induced accumulation of M2 macrophages. In support of this notion, several recent studies have uncovered the eosinophils-type 2 cytokines IL4/13-M2 macrophage circuit as a key component in orchestrating cold-induced development of functional beige cells in subcutaneous fat (Qiu et al., 2014; Rao et al., 2014). In response to cold challenge, IL-4 induces activation of M2 macrophages, which in turn induces the expression of tyrosine hydroxylase for production of catecholamine, a key factor required for browning of WAT. However, it is important to note that cold exposure-induced elevation of *IL-4*/*IL-13* in scWAT is transient, which reaches to the peak level at 24 hr and then declines to below the baseline level at day 6 (Figure S5). On the other hand, massive accumulation of both M2 macrophages and adiponectin continues to increase even after prolonged cold exposure (1 month). Therefore, while recruitment of M2 macrophages in scWAT at the initial phase of cold acclimation is initiated by eosinophils/IL-4, adiponectin is obligatory for sustained presence of M2 in the local tissue during prolonged cold adaptation.

ILC2s, an important player in sustaining eosinophiles and M2 macrophages in adipose tissues, have recently been shown to limit obesity by promoting beige cell biogenesis (Brestoff et al., 2015; Lee et al., 2015a). Lee and colleagues showed that ILC2-derived Th2 cytokines stimulates expansion of bipotential PDGFRα$^+$ progenitor cells and their subsequent commitment to the beige cell lineage. On the other hand, Brestoff et al. (2015) demonstrated that ILC2s promote beiging of scWAT independent of Th2 cytokines by secreting methionine-enkephalin peptides. However, the roles of ILC2s and ILC2-derived cytokines in cold-induced biogenesis have not been explored so far. It is important to note that cold-induced beige cell formation of scWAT was derived primarily from the preexisting unilocular adipocytes, but not the proliferation of bipotential PDGFRα$^+$ progenitors (Lee et al., 2015b). We found that the abundance of ILC2s and its secretory products *IL-5*, *IL-13*, and *Penk* were

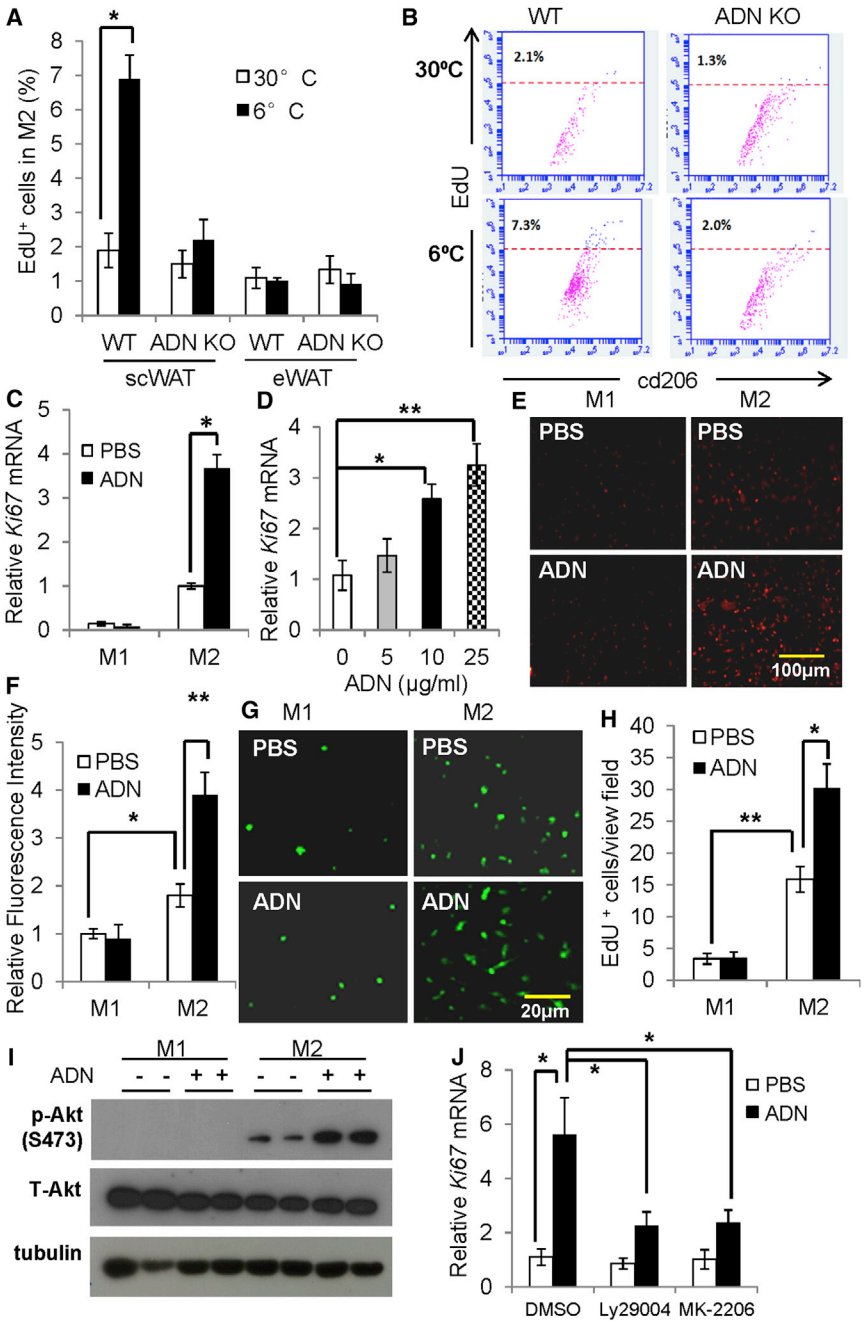

Figure 6. Adiponectin Promoted Cold-Induced Macrophage Proliferation

(A and B) 10-week-old male ADN KO mice and WT littermates with C57BL/6J background were daily injected with EdU (2 mg/kg/day) and housed at 6°C or 30°C for 6 days. (A) Percentage of EdU$^+$ cells in M2 macrophages (as defined by F4/80$^+$cd206$^+$) from scWAT and eWAT as determined by flow cytometry. (B) Representative flowchart images of flow cytometry. The cells above the dotted lines are EdU$^+$ M2 macrophages.

(C–F) Bone marrow-derived macrophages were induced to M1 or M2, followed by treatment with 25 μg/ml adiponectin (ADN) for 24 hr. (C) The mRNA level of *Ki67* in different subtypes of macrophages. (D) Dose-dependent effect of adiponectin on *Ki67* mRNA expression in M2 macrophages. (E) Immunofluorescence staining of Ki67 (scale bar, 100 μm) and (F) quantification of (E).

(G) EdU imaging (scale bar, 20 μm) and (H) EdU$^+$ cells were counted in 8 randomly selected microscopic fields (×40) and were expressed as average number per microscopic field in different subtypes of macrophages.

(I) Western blots of phosho-S473 and total Akt in M1 and M2 macrophages with or without adiponectin treatment (25 μg/ml, 1 hr).

(J) M2 macrophages were pre-incubated with the PI3K inhibitor Ly29004 (20 μM), Akt inhibitor MK-2206 (500 nM), or DMSO as control for 1 hr before addition of recombinant adiponectin (25 μg/ml) for 24 hr. The mRNA expression of *Ki67* was examined by real-time PCR. Data represent mean ± SEM; n = 3 independent experiments; 6 mice or wells for each experiment; *p < 0.05, **p < 0.01. See also Figures S5 and S6.

elevated to various degrees at the early phase of cold challenge but decreased after prolonged cold exposure (6 days). Adiponectin deficiency had no obvious effects on ILC2s and expression of type 2 cytokines, suggesting that Th2 cytokines and ILC2s are not the downstream effectors of adiponectin during cold-induced beiging.

Macrophages are the most abundant cell type in the SVF of adipose tissues, accounting for 10% and 40% in lean and obese states, respectively (Lumeng et al., 2007). The source of adipose tissue-resident macrophages is still a matter of debate. While obesity-induced accumulation of macrophages, which are mainly the pro-inflammatory M1 phenotype, is recruited from the circulating monocytes (Gordon and Taylor, 2005; Oh et al., 2012), the preponderance of macrophages residing in lean adipose tissues exhibit M2 phenotypes and are perhaps from in situ proliferation (Lumeng et al., 2008). Indeed, there is accumulating evidence that tissue-resident macrophages undergo in situ proliferation with minimal contribution from circulating monocytes in several patho-physiological conditions (Hashimoto et al., 2013; Jenkins et al., 2011; Robbins et al., 2013). In the present study, our in vivo cell tracking analysis demonstrated that adiponectin-mediated accumulation of M2 macrophages in cold-stressed scWAT is due to the self-renewal, but not from incorporation of circulating monocytes. This conclusion is also supported by our in vitro data showing the direct stimulatory effects of adiponectin on M2 macrophage proliferation in a T-cadherin/Akt-dependent manner. On the other hand, Qiu et al. demonstrated that cold-induced accumulation of M2 macrophage was abolished in CCR2 KO mice, suggesting that CCR2$^+$ monocytes in circulation are also an important contributor (Qiu et al., 2014). Given the transient nature in cold-induced expression of the chemokine MCP1, we propose

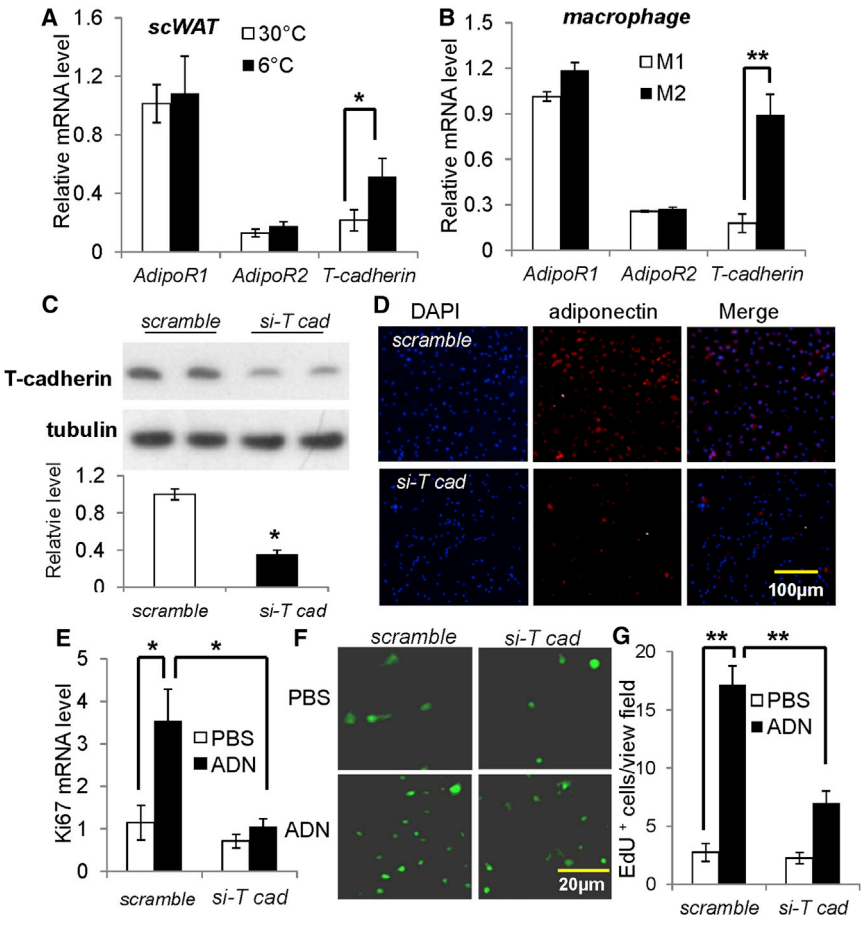

Figure 7. T-Cadherin Was Required for Adiponectin-Induced M2 Macrophage Proliferation

(A) The mRNA level of adiponectin receptor (*adipoR*) *1*, *2*, and *T-cadherin* in scWAT of C57BL/6 mice housed at 6°C or 30°C for 6 days.

(B) The relative mRNA abundance of *adipoR1*, *adipoR2*, and *T-cadherin* in bone marrow-derived M1 and M2 macrophages.

(C–E) Effects of knocking down T-cadherin on adiponectin-induced M2 macrophage proliferation. M2 macrophages were transfected with scramble siRNA (*scramble*) or siRNA targeting endogenous T-cadherin (*si-T cad*) for 24 hr, followed by treatment with adiponectin (ADN) (25 μg/ml) or PBS, and EdU (5 μM) for another 24 hr. (C) Western blot analysis (upper panel) and densitometry quantification (lower panel) of T-cadherin in M2 macrophages at 48 hr after transfection. (D) Cells were immunostained under an unpermeabilized condition for adiponectin bound to the cell surface. Scale bar, 100 μm. (E) The *Ki67* mRNA levels determined by real-time PCR.

(F and G) Representative images for EdU incorporation in (F) M2 macrophages (scale bar, 20 μm) and (G) EdU$^+$ cells were counted in 8 randomly selected microscopic fields (×40) and were expressed as average number per microscopic field. Data represent mean ± SEM; n = 4 independent experiments; 6 mice or wells for each experiment; $^*p < 0.05$, $^{**}p < 0.01$.

that there exists a biphasic accumulation of M2 macrophage in scWAT during cold acclimation: circulating monocytes may contribute to the initial phase of cold-induced accumulation of M2 macrophages, thus enabling a swift supply for catecholamine to initiate the local thermogenesis. Afterward, adiponectin-elicited proliferation becomes the main source for the ensuing maintenance of M2 macrophages. Such a scenario of biphasic mechanism for macrophage enrichment has also been observed during the development of atherosclerotic lesions (Robbins et al., 2013).

The physiological relevance of adiponectin-mediated browning of scWAT with respect to whole-body energy expenditure and metabolic homeostasis needs further clarification. Although the contribution of beige cells to the overall energy expenditure is much smaller than classical BAT, emerging evidence suggests that enhancing the browning of WAT alone is sufficient to reduce obesity in mice (Cohen et al., 2014). Consistently, our present study showed that the impairment of cold-induced browning and thermogenesis in scWAT of ADN KO mice is accompanied by a modest but significant reduction in whole-body energy expenditure. The inverse correlation between plasma adiponectin and body fat has been repeatedly documented in both humans and rodents with obesity (Arita et al., 1999; Lara-Castro et al., 2006). While the prevailing view is that hypoadiponectinemia is the consequence of obesity and is causally involved in the pathogenesis of obesity-induced cardiometabolic diseases (Kadowaki et al., 2006), a number of studies also implicate that reduced plasma adiponectin might be a cause of obesity. ADN KO mice have been shown to be more susceptible to high-fat-diet-induced obesity (Asano et al., 2009; Ouchi et al., 2003), whereas no obvious change in body weight has also been reported in several other studies (Chang et al., 2010). Conversely, peripheral supplementation of recombinant adiponectin caused a profound weight reduction in both dietary and genetic obese mice without affecting food intake (Masaki et al., 2003; Yamauchi et al., 2001). However, despite improved metabolic parameters, mice adipose tissue-selective overexpression of adiponectin in *ob/ob* background are morbidly obese, possibly due to enhanced adipogenesis via PPARγ signaling (Kim et al., 2007). Taken together, these findings highlight a complex role of adiponectin in controlling adiposity via multiple mechanisms, which need further investigation in the future.

In summary, the present study uncovers adiponectin as a novel mediator in adaptive thermogenesis and further supports the obligatory roles of the innate immune system as a local thermogenic efferent during cold-induced browning in scWAT. Apart from the thermogenic activities, brown adipocytes and/or beige cells have several additional metabolic benefits, including glucose and lipid clearance and anti-inflammation (Bartelt et al., 2011; Cohen et al., 2014; Stanford et al., 2013). Therefore, activation of browning and thermogenic program by adiponectin may represent a key mechanism whereby this adipokine defends against various metabolic stresses.

EXPERIMENTAL PROCEDURES

Animals

Adiponectin knockout mice (ADN KO) in C57BL/6J background were generated as described (Hoo et al., 2007). Mice were housed in a controlled environment (12 hr light/dark cycle, 22°C ± 1°C, 60%–70% humidity) and fed ad libitum with standard chow (LabDiet 5053, LabDiet). For cold challenge experiments, 10-week-old male mice were housed in pre-chilled cages (two mice per cage) at 6°C for various time periods. Alternatively, mice were placed at 30°C in a laboratory incubator as thermoneutral controls. All animal experiments were conducted in accordance with the Guidelines of HKU Animal Care and Use Committee.

In Vivo Adiponectin Tracing

The eukaryotically expressed full-length adiponectin was generated as previously described (Xu et al., 2003). 500 μg recombinant adiponectin was labeled with NHS-activated DyLight488 (Thermo Fisher Scientific) at room temperature for 1 hr at dark. The unreacted dye was removed by dialyzing in PBS for 48 hr at 6°C. 50 μg of labeled adiponectin was tail vein injected to ADN KO mouse, and the fluorescence was monitored by the PE IVIS Spectrum in vivo imaging system. The tissues were homogenized in PBS and the fluorescence of tissue lysates was quantified by the Synergy H1 Hybrid Microplate Reader (BioTek).

Indirect Calorimetry

Whole-body oxygen consumption was measured using the comprehensive laboratory animal monitoring system (CLAMS, Columbus Instruments) as described previously (Wong et al., 2014). Briefly, mice were housed singly in CLAMS cages and acclimated for 48 hr, and data on oxygen consumption rate (VO2) were recorded every 18 or 22 min for a 48 hr period with temperature at 22°C or 6°C.

Tissue Oxygen Consumption Rate

Cellular metabolic rates were measured using an XFe24 Analyzer (Seahorse Bioscience). The adipose tissues were cut into 2 mm^3 and pre-incubated in DMEM without $NaHCO_3$ at 37°C for 1 hr before measurement. Oligomycin (ATP synthase inhibitor), 1.4 μM carbonyl cyanide-4-(trifluoromethoxy) phenylhydrazone (FCCP, cellular uncoupler), 2 mM GDP (UCP1 inhibitor), and 10 μM norepinephrine (NE, β3 adrenergic agonist) (Sigma) were sequentially added during the assay to measure the basal, ATP-dependent, maximal, UCP1-dependent, and β3 adrenergic receptor-dependent oxygen consumption, respectively.

Flow Cytometry Analysis of Macrophages in Adipose SVF

The SVF was isolated as described (Ruan et al., 2003), with minor modifications. Briefly, fat pads were digested in 0.1% (w/v) collagenase type I (Invitrogen) for 30 min at 37°C with gentle shaking. The digestion mixture was passed through a 100 μm cell strainer (BD Biosciences) and centrifuged at 800 × *g* for 10 min at 4°C. The SVF pellets were collected and washed twice before staining with antibodies: F4/80-PE (Biolegend, 1:100), cd206 Alexa Fluor 647 (Biolegend, 1:100), cd11c-FITC (Biolegend,1:100), cd11b-FITC (Biolegend, 1:100), lineage-FITC (Biolegend, 1:200), CD45-Pacific Blue (biolegend, 1:100), CD25-PE (BD, 1:100), and IL-33R-AF700 (R&D, 1:100). Species-matched IgG were used as non-specific isotype controls. For flow cytometry analysis of macrophages, 1 × 10^5 freshly isolated cells were triple stained with F4/80 PE (1:100), cd206 Alexa Fluor 647 (1:100), cd11c FITC or cd11c Cy7 (1:100), or their isotype controls (Biolegend) on ice for 30 min in dark. For analysis of ILC2s, 2 × 10^5 freshly isolated cells were stained with lineage markers: FITC (Biolegend, 1:200), CD45-Pacific Blue (biolegend, 1:100), CD25-PE (BD, 1:100), and IL-33R-AF700 (R&D, 1:100). For FACS analysis of EdU^+ cells, freshly isolated SVCs were processed for Click-iT Reaction (Invitrogen), followed by staining with cell-surface marker F4/80, cd11c, and cd206. After washing, the cells were fixed in 4% formalin and analyzed with FXP-500 flow cytometer (Beckman) (for macrophage) and BD LSRFortessa Cell Analyzer (BD) (for ILC2s).

In Vivo Monocyte/Macrophage Tracking

Peripheral blood of 10-week-old C57BL/6J male mice was collected to heparinized tubes (Fisher) and incubated with 9 volumes of the erythrocyte lysis buffer (0.15 M NH_4Cl, 10 mM $KHCO_3$, 0.1 mM EDTA) for 10 min on ice. After that, monocytes were isolated from the leukocytes with the EasySep mouse monocyte enrichment kit (Stemcell Tech) and subsequently labeled with the PKH26 labeling kit (Sigma) at a concentration of 2 mM for 1 min. 1 × 10^6 labeled cells were injected to each recipient mouse via tail vein. After 2 hr of recovery, the mice were housed at 6°C for 72 hr, and the cells in blood and in various tissues were stained for cd11b FITC and subjected to flow cytometry analysis for the presence of $PKH26^+$ myeloid cells.

Cell Culture

Bone marrow cells were isolated from the femur and tibia of C57BL/6J mice and differentiated to mature macrophages for 7 days as described (Weischenfeldt and Porse, 2008). On day 8, differentiated macrophages were polarized to either M1 (100 ng/ml IFN-γ, Peprotech, plus 10 ng/ml LPS, Sigma) or M2 (10 ng/ml IL-4, Peprotech) for 48 hr before incubation with recombinant adiponectin. For EdU incorporation, 5 μM EdU (Invitrogen) was added to the macrophages along with adiponectin (Invitrogen). For knocking down *T-cadherin*, M2 macrophages were transfected with siRNA targeting *T-cadherin* or scrambled siRNA (Raybio) using Lipofectamine 2000 (Invitrogen) and incubated for 24 hr before the addition of adiponectin.

Real-Time PCR and Western Blot Analysis

Total RNA was extracted by Trizol (Invitrogen) and reverse transcribed into cDNA using the ImProm-II reverse transcriptase (Promega). Real-time PCR reactions were performed using SYBR Green master mix (Invitrogen) on a 7900 HT (Applied Biosystems), normalized with the *Gapdh* gene. See Table S1 for the primer sequences. Proteins were extracted from tissues or cells in RIPA buffer (0.5% NP40, 0.1% sodium deoxycholate, 150 mM NaCl, 50 mM TrisHCl [pH 7.4]) containing complete protease inhibitor cocktail (Roche). PVDF membrane was probed with primary antibodies UCP1 (Abcam), Akt (Cell Signaling Technology), β tubulin (Cell Signaling Technology), phospho-Akt (S473), T cadherin (Abcam), and adiponectin (Antibody and Immunoassay Services, the University of Hong Kong [AIS, HKU]). The protein bands were visualized with enhanced chemiluminescence reagents (GE Healthcare) and quantified using the NIH ImageJ software.

Histological, Immunohistochemical, and Biochemical Analysis

Adipose tissues were fixed in 10% formalin solution for 24 hr, embedded in paraffin, and sectioned at 5 μm. Deparaffinized and dehydrated sections were incubated with affinity-purified rabbit antibody against mouse adiponectin (AIS, HKU), rabbit antibody against mouse UCP1 (Abcam) in PBS containing 3% BSA overnight at 4°C, followed by incubation with a horseradish peroxidase-conjugated secondary antibody against rabbit IgG (Cell Signaling Technology), and developed by SIGMAFAST DAB (Sigma). For immunocytochemical staining, bone marrow-derived macrophages were fixed in ice-cold 4% formaldehyde for 10 min. The cells were then incubated with antibody against Ki67 (Abcam) or adiponectin in PBS containing 3% BSA overnight at 4°C, washed and incubated with fluorochrome-conjugated secondary antibodies (Alexa Fluor 555 anti-rabbit, Molecular Probes), and diluted in PBS for 1 hr at room temperature at dark. Slides were counterstained with DAPI. Tissue sections and cell slides were visualized with an Olympus biological microscope BX41, and images were captured with an Olympus DP72 color digital camera. Adiponectin levels in serum were measured by mouse adiponectin ELISA kit (AIS, HKU).

Statistical Analysis

All analyses were performed with Statistical Package for Social Sciences version 14.0 (SPSS). Data were expressed as mean ± SEM. Statistical significance was determined by Student's t test (for comparison of two experimental conditions) or ANOVA (for comparison of three or more experimental conditions). Comparisons with $p < 0.05$ were considered statistically significant.

SUPPLEMENTAL INFORMATION

Supplemental Information includes six figures and one table and can be found with this article online at http://dx.doi.org/10.1016/j.cmet.2015.06.004.

AUTHOR CONTRIBUTIONS

X.H. designed the study, carried out the research, analyzed and interpreted the results, and wrote the manuscript. P.G. designed the study, carried out the

research, and analyzed the results. J.Z., T.N., Y.P., T.F., and C.Z. conducted the experiments. D.W., Y.W., and K.S.L.L. reviewed the manuscript. A.X. designed the study and wrote and edited the manuscript.

ACKNOWLEDGMENTS

This work was supported by National 973 Basic Research Program of China (2015CB553603), Research grant council of Hong Kong (17124714 and C7055-14G), HKU matching fund for the state key laboratory of Pharmaceutical Biotechnology, and the National Natural Science Foundation of China (81300658).

Received: January 13, 2015
Revised: April 22, 2015
Accepted: June 9, 2015
Published: July 9, 2015

REFERENCES

Arita, Y., Kihara, S., Ouchi, N., Takahashi, M., Maeda, K., Miyagawa, J., Hotta, K., Shimomura, I., Nakamura, T., Miyaoka, K., et al. (1999). Paradoxical decrease of an adipose-specific protein, adiponectin, in obesity. Biochem. Biophys. Res. Commun. *257*, 79–83.

Asano, T., Watanabe, K., Kubota, N., Gunji, T., Omata, M., Kadowaki, T., and Ohnishi, S. (2009). Adiponectin knockout mice on high fat diet develop fibrosing steatohepatitis. J. Gastroenterol. Hepatol. *24*, 1669–1676.

Awad, E.M., Khan, S.Y., Sokolikova, B., Brunner, P.M., Olcaydu, D., Wojta, J., Breuss, J.M., and Uhrin, P. (2013). Cold induces reactive oxygen species production and activation of the NF-kappa B response in endothelial cells and inflammation in vivo. J. Thromb. Haemost. *11*, 1716–1726.

Bartelt, A., Bruns, O.T., Reimer, R., Hohenberg, H., Ittrich, H., Peldschus, K., Kaul, M.G., Tromsdorf, U.I., Weller, H., Waurisch, C., et al. (2011). Brown adipose tissue activity controls triglyceride clearance. Nat. Med. *17*, 200–205.

Brestoff, J.R., Kim, B.S., Saenz, S.A., Stine, R.R., Monticelli, L.A., Sonnenberg, G.F., Thome, J.J., Farber, D.L., Lutfy, K., Seale, P., and Artis, D. (2015). Group 2 innate lymphoid cells promote beiging of white adipose tissue and limit obesity. Nature *519*, 242–246.

Cannon, B., and Nedergaard, J. (2004). Brown adipose tissue: function and physiological significance. Physiol. Rev. *84*, 277–359.

Cawthorn, W.P., Scheller, E.L., Learman, B.S., Parlee, S.D., Simon, B.R., Mori, H., Ning, X., Bree, A.J., Schell, B., Broome, D.T., et al. (2014). Bone marrow adipose tissue is an endocrine organ that contributes to increased circulating adiponectin during caloric restriction. Cell Metab. *20*, 368–375.

Chang, J., Li, Y., Huang, Y., Lam, K.S., Hoo, R.L., Wong, W.T., Cheng, K.K., Wang, Y., Vanhoutte, P.M., and Xu, A. (2010). Adiponectin prevents diabetic premature senescence of endothelial progenitor cells and promotes endothelial repair by suppressing the p38 MAP kinase/p16INK4A signaling pathway. Diabetes *59*, 2949–2959.

Cohen, P., Levy, J.D., Zhang, Y., Frontini, A., Kolodin, D.P., Svensson, K.J., Lo, J.C., Zeng, X., Ye, L., Khandekar, M.J., et al. (2014). Ablation of PRDM16 and beige adipose causes metabolic dysfunction and a subcutaneous to visceral fat switch. Cell *156*, 304–316.

Cypess, A.M., Lehman, S., Williams, G., Tal, I., Rodman, D., Goldfine, A.B., Kuo, F.C., Palmer, E.L., Tseng, Y.H., Doria, A., et al. (2009). Identification and importance of brown adipose tissue in adult humans. N. Engl. J. Med. *360*, 1509–1517.

Denzel, M.S., Scimia, M.C., Zumstein, P.M., Walsh, K., Ruiz-Lozano, P., and Ranscht, B. (2010). T-cadherin is critical for adiponectin-mediated cardioprotection in mice. J. Clin. Invest. *120*, 4342–4352.

Dietrich, M.O., and Horvath, T.L. (2012). Limitations in anti-obesity drug development: the critical role of hunger-promoting neurons. Nat. Rev. Drug Discov. *11*, 675–691.

Dong, M., Yang, X., Lim, S., Cao, Z., Honek, J., Lu, H., Zhang, C., Seki, T., Hosaka, K., Wahlberg, E., et al. (2013). Cold exposure promotes atherosclerotic plaque growth and instability via UCP1-dependent lipolysis. Cell Metab. *18*, 118–129.

Gordon, S., and Taylor, P.R. (2005). Monocyte and macrophage heterogeneity. Nat. Rev. Immunol. *5*, 953–964.

Hashimoto, D., Chow, A., Noizat, C., Teo, P., Beasley, M.B., Leboeuf, M., Becker, C.D., See, P., Price, J., Lucas, D., et al. (2013). Tissue-resident macrophages self-maintain locally throughout adult life with minimal contribution from circulating monocytes. Immunity *38*, 792–804.

Hoo, R.L., Chow, W.S., Yau, M.H., Xu, A., Tso, A.W., Tse, H.F., Fong, C.H., Tam, S., Chan, L., and Lam, K.S. (2007). Adiponectin mediates the suppressive effect of rosiglitazone on plasminogen activator inhibitor-1 production. Arterioscler. Thromb. Vasc. Biol. *27*, 2777–2782.

Hug, C., Wang, J., Ahmad, N.S., Bogan, J.S., Tsao, T.S., and Lodish, H.F. (2004). T-cadherin is a receptor for hexameric and high-molecular-weight forms of Acrp30/adiponectin. Proc. Natl. Acad. Sci. USA *101*, 10308–10313.

Jenkins, S.J., Ruckerl, D., Cook, P.C., Jones, L.H., Finkelman, F.D., van Rooijen, N., MacDonald, A.S., and Allen, J.E. (2011). Local macrophage proliferation, rather than recruitment from the blood, is a signature of TH2 inflammation. Science *332*, 1284–1288.

Joshi, M.B., Philippova, M., Ivanov, D., Allenspach, R., Erne, P., and Resink, T.J. (2005). T-cadherin protects endothelial cells from oxidative stress-induced apoptosis. FASEB J. *19*, 1737–1739.

Kadowaki, T., Yamauchi, T., Kubota, N., Hara, K., Ueki, K., and Tobe, K. (2006). Adiponectin and adiponectin receptors in insulin resistance, diabetes, and the metabolic syndrome. J. Clin. Invest. *116*, 1784–1792.

Kim, J.Y., van de Wall, E., Laplante, M., Azzara, A., Trujillo, M.E., Hofmann, S.M., Schraw, T., Durand, J.L., Li, H., Li, G., et al. (2007). Obesity-associated improvements in metabolic profile through expansion of adipose tissue. J. Clin. Invest. *117*, 2621–2637.

Lara-Castro, C., Luo, N., Wallace, P., Klein, R.L., and Garvey, W.T. (2006). Adiponectin multimeric complexes and the metabolic syndrome trait cluster. Diabetes *55*, 249–259.

Lee, M.W., Odegaard, J.I., Mukundan, L., Qiu, Y., Molofsky, A.B., Nussbaum, J.C., Yun, K., Locksley, R.M., and Chawla, A. (2015a). Activated type 2 innate lymphoid cells regulate beige fat biogenesis. Cell *160*, 74–87.

Lee, Y.H., Petkova, A.P., Konkar, A.A., and Granneman, J.G. (2015b). Cellular origins of cold-induced brown adipocytes in adult mice. FASEB J. *29*, 286–299.

Lin, Z., Wu, F., Lin, S., Pan, X., Jin, L., Lu, T., Shi, L., Wang, Y., Xu, A., and Li, X. (2014). Adiponectin protects against acetaminophen-induced mitochondrial dysfunction and acute liver injury by promoting autophagy in mice. J. Hepatol. *61*, 825–831.

Lumeng, C.N., Bodzin, J.L., and Saltiel, A.R. (2007). Obesity induces a phenotypic switch in adipose tissue macrophage polarization. J. Clin. Invest. *117*, 175–184.

Lumeng, C.N., DelProposto, J.B., Westcott, D.J., and Saltiel, A.R. (2008). Phenotypic switching of adipose tissue macrophages with obesity is generated by spatiotemporal differences in macrophage subtypes. Diabetes *57*, 3239–3246.

Mandal, P., Pratt, B.T., Barnes, M., McMullen, M.R., and Nagy, L.E. (2011). Molecular mechanism for adiponectin-dependent M2 macrophage polarization: link between the metabolic and innate immune activity of full-length adiponectin. J. Biol. Chem. *286*, 13460–13469.

Masaki, T., Chiba, S., Yasuda, T., Tsubone, T., Kakuma, T., Shimomura, I., Funahashi, T., Matsuzawa, Y., and Yoshimatsu, H. (2003). Peripheral, but not central, administration of adiponectin reduces visceral adiposity and upregulates the expression of uncoupling protein in agouti yellow (Ay/a) obese mice. Diabetes *52*, 2266–2273.

Nakatsuji, H., Kishida, K., Sekimoto, R., Komura, N., Kihara, S., Funahashi, T., and Shimomura, I. (2014). Accumulation of adiponectin in inflamed adipose tissues of obese mice. Metabolism *63*, 542–553.

Nedergaard, J., Golozoubova, V., Matthias, A., Asadi, A., Jacobsson, A., and Cannon, B. (2001). UCP1: the only protein able to mediate adaptive

non-shivering thermogenesis and metabolic inefficiency. Biochim. Biophys. Acta *1504*, 82–106.

Oh, D.Y., Morinaga, H., Talukdar, S., Bae, E.J., and Olefsky, J.M. (2012). Increased macrophage migration into adipose tissue in obese mice. Diabetes *61*, 346–354.

Ouchi, N., Ohishi, M., Kihara, S., Funahashi, T., Nakamura, T., Nagaretani, H., Kumada, M., Ohashi, K., Okamoto, Y., Nishizawa, H., et al. (2003). Association of hypoadiponectinemia with impaired vasoreactivity. Hypertension *42*, 231–234.

Parker-Duffen, J.L., Nakamura, K., Silver, M., Kikuchi, R., Tigges, U., Yoshida, S., Denzel, M.S., Ranscht, B., and Walsh, K. (2013). T-cadherin is essential for adiponectin-mediated revascularization. J. Biol. Chem. *288*, 24886–24897.

Qiu, Y., Nguyen, K.D., Odegaard, J.I., Cui, X., Tian, X., Locksley, R.M., Palmiter, R.D., and Chawla, A. (2014). Eosinophils and type 2 cytokine signaling in macrophages orchestrate development of functional beige fat. Cell *157*, 1292–1308.

Rao, R.R., Long, J.Z., White, J.P., Svensson, K.J., Lou, J., Lokurkar, I., Jedrychowski, M.P., Ruas, J.L., Wrann, C.D., Lo, J.C., et al. (2014). Meteorin-like is a hormone that regulates immune-adipose interactions to increase beige fat thermogenesis. Cell *157*, 1279–1291.

Robbins, C.S., Hilgendorf, I., Weber, G.F., Theurl, I., Iwamoto, Y., Figueiredo, J.L., Gorbatov, R., Sukhova, G.K., Gerhardt, L.M., Smyth, D., et al. (2013). Local proliferation dominates lesional macrophage accumulation in atherosclerosis. Nat. Med. *19*, 1166–1172.

Rosen, E.D., and Spiegelman, B.M. (2014). What we talk about when we talk about fat. Cell *156*, 20–44.

Ruan, H., Zarnowski, M.J., Cushman, S.W., and Lodish, H.F. (2003). Standard isolation of primary adipose cells from mouse epididymal fat pads induces inflammatory mediators and down-regulates adipocyte genes. J. Biol. Chem. *278*, 47585–47593.

Rückerl, D., Jenkins, S.J., Laqtom, N.N., Gallagher, I.J., Sutherland, T.E., Duncan, S., Buck, A.H., and Allen, J.E. (2012). Induction of IL-4Rα-dependent microRNAs identifies PI3K/Akt signaling as essential for IL-4-driven murine macrophage proliferation in vivo. Blood *120*, 2307–2316.

Seale, P., Bjork, B., Yang, W., Kajimura, S., Chin, S., Kuang, S., Scimè, A., Devarakonda, S., Conroe, H.M., Erdjument-Bromage, H., et al. (2008). PRDM16 controls a brown fat/skeletal muscle switch. Nature *454*, 961–967.

Stanford, K.I., Middelbeek, R.J., Townsend, K.L., An, D., Nygaard, E.B., Hitchcox, K.M., Markan, K.R., Nakano, K., Hirshman, M.F., Tseng, Y.H., and Goodyear, L.J. (2013). Brown adipose tissue regulates glucose homeostasis and insulin sensitivity. J. Clin. Invest. *123*, 215–223.

Weischenfeldt, J., and Porse, B. (2008). Bone Marrow-Derived Macrophages (BMM): Isolation and Applications. CSH Protoc *2008*, t5080.

Wong, C.M., Wang, Y., Lee, J.T., Huang, Z., Wu, D., Xu, A., and Lam, K.S. (2014). Adropin is a brain membrane-bound protein regulating physical activity via the NB-3/Notch signaling pathway in mice. J. Biol. Chem. *289*, 25976–25986.

Wu, J., Boström, P., Sparks, L.M., Ye, L., Choi, J.H., Giang, A.H., Khandekar, M., Virtanen, K.A., Nuutila, P., Schaart, G., et al. (2012). Beige adipocytes are a distinct type of thermogenic fat cell in mouse and human. Cell *150*, 366–376.

Xu, A., Wang, Y., Keshaw, H., Xu, L.Y., Lam, K.S., and Cooper, G.J. (2003). The fat-derived hormone adiponectin alleviates alcoholic and nonalcoholic fatty liver diseases in mice. J. Clin. Invest. *112*, 91–100.

Yamauchi, T., Kamon, J., Waki, H., Terauchi, Y., Kubota, N., Hara, K., Mori, Y., Ide, T., Murakami, K., Tsuboyama-Kasaoka, N., et al. (2001). The fat-derived hormone adiponectin reverses insulin resistance associated with both lipoatrophy and obesity. Nat. Med. *7*, 941–946.

Yamauchi, T., Kamon, J., Ito, Y., Tsuchida, A., Yokomizo, T., Kita, S., Sugiyama, T., Miyagishi, M., Hara, K., Tsunoda, M., et al. (2003). Cloning of adiponectin receptors that mediate antidiabetic metabolic effects. Nature *423*, 762–769.

Ye, L., Wu, J., Cohen, P., Kazak, L., Khandekar, M.J., Jedrychowski, M.P., Zeng, X., Gygi, S.P., and Spiegelman, B.M. (2013). Fat cells directly sense temperature to activate thermogenesis. Proc. Natl. Acad. Sci. USA *110*, 12480–12485.